Parameter Uniqueness and Uncertainty Associated with Multirate Transport Models Applied to Core-Scale Test Data

Kristopher L. Kuhlman[1] klkuhlm@sandia.gov, Bwalya Malama[1] bnmalam@sandia.gov, Scott C. James[2] scjames@sandia.gov; AGU Fall Meeting 2011 H31D-1179
[1] Repository Performance Dept. Sandia National Laboratories†, Carlsbad, NM; [2] Thermal/Fluid Science Dept. Sandia National Laboratories†, Livermore, CA

The hydrology and transport characteristics of the Culebra Dolomite Member of the Permian Rustler Formation have been extensively studied due to this unit's role as a potential long-term radionuclide transport pathway from the Waste Isolation Pilot Plant (WIPP) to the accessible environment. Hundreds of hydraulic tests and several large-scale tracer tests have been conducted in the Culebra in the vicinity of the WIPP. The tracer tests have revealed that the multiple scales of porosity observed in the Culebra (Figure 1) lead to transport breakthrough concentration profiles that cannot be adequately simulated using single-rate or double-porosity models [Haggerty et al., 2001].

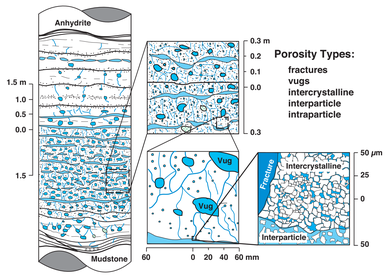

Fig 1. *Culebra Dolomite porosity types*

The long-tail breakthrough curves in field-scale Culebra tracer tests have been confirmed through two large-scale tracer tests in the mid 1990's [Haggerty et al., 2000]. Alternatively, it has been hypothesized that parameter heterogeneity alone could be used to explain long-tail breakthroughs observed [Altman et al., 2002], but the multirate model is superior in its ability to recreate tracer breakthrough data at the field scale.
Large horizontal Culebra cores (see photographs in Figure 2) were collected to perform controlled laboratory radionuclide tracer tests [Lucero et al., 1998].

The results from these tests were originally analyzed using only single- and double-porosity models; the authors use of single-porosity models for core-scale transport were at variance with the use of multirate transport models to analyze field-scale data.

Core-Scale Transport Tests

In this work, we have re-interpreted the column-scale tracer tests using a modified form of a multirate transport model, which was also used at the field scale. We conclude that the multirate model yields superior fits to the observed core-scale breakthrough data; our use of the multirate model is in line with that used previously to interpret field-scale data.

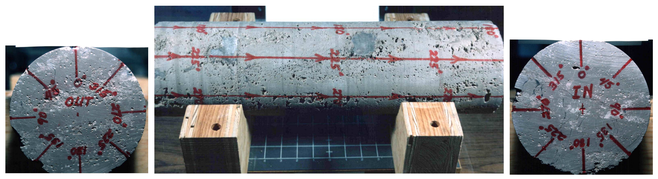

Fig 2. *50.9-cm core with vuggy porosity, fractures, and pore-filling calcite; inch grid in foreground.*

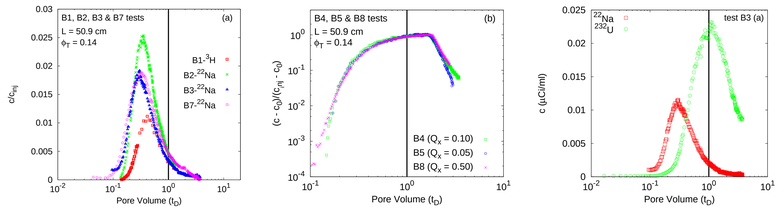

Fig 3. *Breakthrough data for column study; vertical lines are 1 pore volume based on total porosity (ϕ_{total}) of 0.14. c_{inj} is the injectate concentration, while c_0 is the initial background concentration.*

Multirate Solute Transport Model

The multirate mass transfer model conceives of the transport domain as two overlapping continua, the mobile (advective or fracture porosity) and immobile (diffusion dominated matrix porosity) zones. Mass exchange between these two domains is governed by a rate-transfer coefficient that is a random variable. Transport of a sorbing radionuclide in the mobile domain is governed by the one-dimensional transport equation [Haggerty and Gorelick, 1995]

$$\frac{\partial c}{\partial t} + \int_0^\infty \beta(\omega)\left(\frac{\partial \langle c_{\text{im}}\rangle}{\partial t} + \lambda \langle c_{\text{im}}\rangle\right) \mathrm{d}\omega = D_R \frac{\partial^2 c}{\partial x^2} - v_R \frac{\partial c}{\partial x} - \lambda c,$$

where c and c_{im} are mobile- and immobile-phase solute concentrations [M L^{-3}], ω is the first-order mass transfer rate coefficient [T^{-1}] as a continuous random variable, $\beta(\omega) = \beta_T p(\omega)$ is the point capacity ratio of the rock matrix [T], $\beta_T = \phi_{\text{im}} R_{\text{im}}/\phi_{\text{m}} R_{\text{m}}$ is the total capacity ratio of the rock matrix, $p(\omega)$ is the distribution function of ω [T], $D_R = D/R_{\text{m}}$, D is the dispersion coefficient [L^2 T^{-1}], $v_R = v/R_{\text{m}}$, v is the average linear velocity [L T^{-1}], ϕ_{m} and ϕ_{im} are the mobile- and immobile-domain porosities, R_{m} and R_{im} are the mobile- and immobile-domain retardation factors, and λ is the first-order radioactive decay constant [T^{-1}]. Transport of a sorbing solute in one-dimension in the immobile zone is governed by

$$\frac{\partial \langle c_{\text{im}}\rangle}{\partial t} = \omega\left(c - \langle c_{\text{im}}\rangle\right) - \lambda \langle c_{\text{im}}\rangle,$$

where $\omega = 2\gamma D_{\text{m}}/(R_{\text{im}} b^2)$ is the mass transfer rate coefficient, D_{m} is the free-water diffusion coefficient, b is the block-length in the immobile domain, $\langle\rangle$ indicates an averaged quantity, and γ is a proportionality constant. We use the lognormal distribution for $\omega_D = \omega L/v_R$ (the Damköhler-I number), where L is column length and the distribution is given by

$$p(\omega_D) = \frac{1}{\omega_D \sigma\sqrt{2\pi}} \exp\left[-\left(\frac{\log(\omega_D) - \mu}{\sigma\sqrt{2}}\right)^2\right],$$

where μ and σ are the mean and standard deviation of $\log(\omega_D)$.

Simulation of Breakthrough Data

The measured breakthrough data were fit with multirate, single-porosity, and double-porosity models using PEST [Doherty, 2009]. Figure 4 shows the fits with both linear (a) or log-scale (b) concentrations.

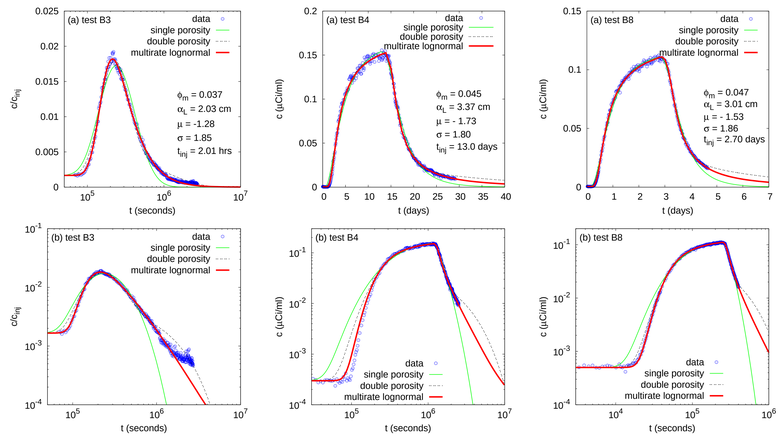

Fig. 4 *Model fit to Culebra core breakthrough data for ^{22}Na tests.*

Parameter Uniqueness and Uncertainty

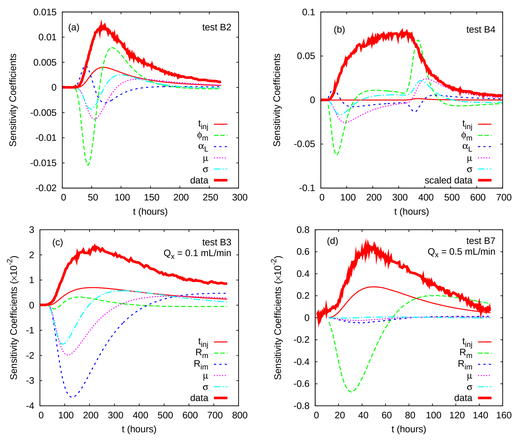

Fig. 5 *PEST-computed parameter sensitivities through time. Q_x is the test flowrate.*

Figure 5 shows the relative sensitivities of estimated parameters during the tests for a short-duration (a) and a long-duration (b) ^{22}Na test. These figures show that the largest sensitivities are associated with changes in input concentration (increases or decreases). Figure 5 also shows low-flow (c) and a high-flow (d) ^{232}U tests. The sensitivity of the immobile-domain retardation factor (R_{im}) and multirate model distribution parameters (μ and σ) are high in (c) and relatively low in (d), where the mobile-domain retardation factor (R_{m}) has high sensitivity. This dependence of sensitivities on flowrates is related to the proportionality between mass transfer and advective transport (i.e., the dimensionless Damköhler-I number).

The Markov-chain Monte Carlo (MCMC) optimization algorithm DREAM [Vrugt et al., 2009] was used to estimate the posterior probability distributions for two long-pulse ^{22}Na tests (B4 and B8 – see Figure 4 for data). The single marginal distributions are shown in Figure 6; the well-defined nearly-Gaussian distributions indicate that all 7 parameters are estimable at the same time from the breakthrough data.

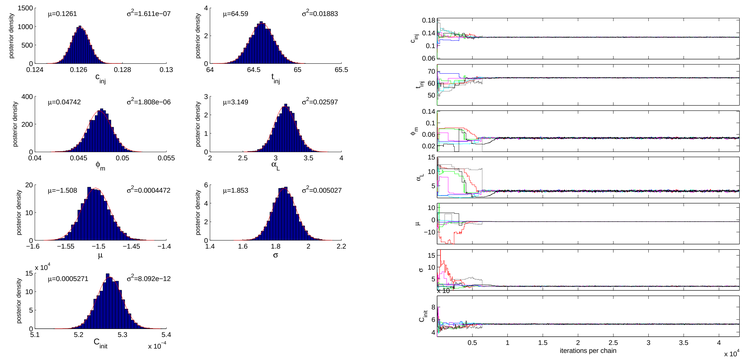

Fig. 6 *DREAM-computed results for ^{22}Na-test B8. Posterior parameter distributions (left) and evolution of chains showing convergence at about 10,000 iterations per chain (right).*

The two-parameter marginal distributions for B4 and B8 are shown in Figure 7; most parameters are at least slightly correlated. The mobile-domain porosity ϕ_{m} and the dispersivity α_L are highly correlated (narrow linear scatterplot blob), while the length of the injection pulse t_{inj} and the initial concentration c_0 are nearly uncorrelated (nearly spherical scatterplot blob). In general, test B8 (flow rate 0.5 ml/min) has less-correlated parameters than B4 (0.1 ml/min), which conceptually agrees with the changes in parameter sensitivity with flowrate observed in Figure 5.

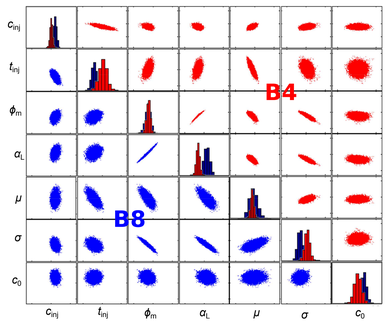

Fig. 7 *DREAM-based two-parameter pairs of posterior parameter estimates for both B4 and B8. Diagonal shows same scaled marginal posterior parameter distributions as in Figure 6, while off-diagonals show relationships between parameters*

Table 1. *Parameter estimates for models fit to conservative tracer tests, some shown in Figure 4.*

Test Q_x (mL/min)	Model	ϕ_{m}	α_L (cm)	ω_D	μ	σ
B1 ^{3}H	Single	0.081	7.99			
	Double	0.073	4.83	0.735		
0.1	Multi	0.060	2.98		-0.498	1.28
B2 ^{22}Na	Single	0.065	7.30			
	Double	0.061	5.14	0.538		
0.1	Multi	0.042	2.18		-1.22	1.98
B3 ^{22}Na	Single	0.062	8.55			
	Double	0.058	6.04	0.395		
0.1	Multi	0.037	2.03		-1.28	1.85
B4 ^{22}Na	Single	0.065	17.5			
	Double	0.062	9.38	0.209		
0.1	Multi	0.045	3.37		-1.73	1.80
B5 ^{22}Na	Single	0.070	16.4			
	Double	0.069	10.7	0.229		
0.05	Multi	0.051	5.72		-1.69	2.10
B7 ^{22}Na	Single	0.071	14.3			
	Double	0.066	9.89	0.473		
0.5	Multi	0.061	8.46		-0.921	0.831
B8 ^{22}Na	Single	0.068	12.9			
	Double	0.065	7.01	0.289		
0.5	Multi	0.047	3.01		-1.53	1.86

Table 1 shows that the multirate model produces more physically realistic dispersivity values (α_L) for a core-size problem (2cm), and mobile porosities (ϕ_m) are also consistently lower. The distribution parameters (μ and σ) for the multirate model are consistent between most of the ^{22}Na tests (except B7). The multirate model is more physically realistic than the single- or double-porosity model for the Culebra Dolomite, based on field-scale testing. Reinterpretation of these core-scale data shows that this is not only true at the field scale; multirate transport can be observed at the centimeter-scale as well as at the meter scale in tracer tests performed at WIPP wells H-19 and H-11 [Meigs et al., 2000].

† Sandia National Laboratories is a multi-program laboratory managed and operated by Sandia Corporation, a wholly owned subsidiary of Lockheed Martin Corporation, for the U.S. Department of Energy's National Nuclear Security Administration under contract DE-AC04-94AL85000. This document is SAND2011-9041P. This research is funded by WIPP programs administered by the Office of Environmental Management (EM) of the US Department of Energy.

S. J. Altman, L. C. Meigs, T. L. Jones, and S. A. McKenna. Controls of mass recovery rates in single-well injection-withdrawal tracer tests with a single-porosity, heterogeneous conceptualization. *Water Resources Research*, 38(7), 2002.

J. Doherty. *PEST User Manual: Model-independent parameter estimation*. Watermark Numerical Computing, Brisbane, Australia, fifth edition, 2009.

R. Haggerty and S. M. Gorelick. Multiple-rate mass transfer for modeling diffusion and surface reactions in media with pore-scale heterogeneity. *Water Resources Research*, 31(10):2383–2400, 1995.

R. Haggerty, S. A. McKenna, and L. C. Meigs. On the late-time behavior of tracer test breakthrough curves. *Water Resources Research*, 36(12):3467–3479, 2000.

R. Haggerty, S. W. Fleming, L. C. Meigs, and S. A. McKenna. Tracer tests in a fractured dolomite: 2. analysis of mass transfer in single-well injection-withdrawal test. *Water Resources Research*, 37(5): 1129–1142, 2001.

D. A. Lucero, G. O. Brown, and C. H. Heath. Laboratory column experiments for radionuclide adsorption studies of the Culebra Dolomite Member of the Rustler Formation. Sandia Report SAND97–1763, Sandia National Laboratories, Albuquerque, NM, 1998.

L. C. Meigs, R. L. Beauheim, and T. L. Jones. Interpretations of tracer tests performed in the Culebra Dolomite at the Waste Isolation Pilot Plant site. Sandia Report SAND97–3109, Sandia National Laboratories, Albuquerque, NM, 2000.

J. A. Vrugt, C. J. F. ter Braak, C. G. H. Diks, D. Higdon, B. A. Robinson, and J. M. Hyman. Accelerating Markov chain Monte Carlo simulation by differential evolution with self-adaptive randomized subspace sampling. *International Journal of Nonlinear Sciences and Numerical Simulation*, 10(3):273–290, 2009.